Inorg. Chem. **2008**, *47*, 9400−9409

Trinuclear Mo_3S_7 Clusters Coordinated to Dithiolate or Diselenolate Ligands and Their Use in the Preparation of Magnetic Single Component Molecular Conductors

Rosa Llusar,*,† Sonia Triguero,† Victor Polo,† Cristian Vicent,*,‡ Carlos J. Gómez-García,§ Olivier Jeannin,|| and Marc Fourmigué||

Departament de Química Física i Analítica, Universitat Jaume I, Campus de Riu Sec, Avda. Sos Baynat s/n, E- 12071 Castelló, Spain, Serveis Centrals d'Instrumentació Cientifica, Universitat Jaume I, Campus de Riu Sec, Avda. Sos Baynat s/n, E- 12071 Castelló, Spain, Instituto de Ciencia Molecular, Universitat de Valencia, Polígono la Coma s/n, E-46980, Paterna, Spain, and Sciences Chimiques de Rennes, Université Rennes 1, UMR CNRS 6226, Campus de Beaulieu, 35042 Rennes, France

Received May 26, 2008

A general route for the preparation of a series of dianionic Mo_3S_7 cluster complexes bearing dithiolate or diselenolate ligands, namely, $[Mo_3S_7L_3]^{2-}$ (where L = tfd (bis(trifluoromethyl)-1,2-dithiolate) ($\mathbf{4}^{2-}$), bdt (1,2-benzenedithiolate) ($\mathbf{5}^{2-}$), dmid (1,3-dithia-2-one-4,5-dithiolate) ($\mathbf{6}^{2-}$), and dsit (1,3-dithia-2-thione-4,5-diselenolate) ($\mathbf{7}^{2-}$)) is reported by direct reaction of $[Mo_3S_7Br_6]^{2-}$ and $(n\text{-Bu})_2$Sn(dithiolate). The redox properties, molecular structure, and electronic structure (BP86/VTZP) of the $\mathbf{4}^{2-}$ to $\mathbf{7}^{2-}$ clusters have also been investigated. The HOMO orbital in all complexes is delocalized over the ligand and the Mo_3S_7 cluster core. Ligand contributions to the HOMO range from 61.67% for $\mathbf{4}^{2-}$ to 82.07% for $\mathbf{7}^{2-}$, which would allow fine-tuning of the electronic and magnetic properties. These dianionic clusters present small energy gaps between the HOMO and HOMO−1 orbitals (0.277−0.104 eV). Complexes $\mathbf{6}^{2-}$ and $\mathbf{7}^{2-}$ are oxidized to the neutral state to afford microcrystalline or amorphous fine powders that exhibit semiconducting behavior and present antiferromagnetic exchange interactions. These compounds are new examples of the still rare single-component conductors based on cluster magnetic units.

Introduction

Metal dithiolene complexes have been extensively investigated because of their combination of functional properties, specific geometries, and intermolecular interactions that confer them an enormous interest in the field of magnetism,[1,2] conductivity,[3−6] and nonlinear optics.[7,8] A great deal on work has been focused on the series of anionic square-planar or tetrahedral homoleptic mononuclear $[M(dithiolene)_2]^{n-}$ (n = 1,2; M = Ni, Pd, Pt, Au, Co, Cu) complexes acting as counterions in charge transfer solids with a variety of donor molecules.[4] These salts display unconventional electrical and magnetic properties that include ferromagnetism, metallic, and superconducting properties. Regarding their neutral counterparts of general formula $M(dithiolene)_2$, Canadell's group envisioned that this class of molecules are expected to match the adequate electronic and structural requirements to internally promote electron transfer between two types of bands leading to single-component molecular metals.[9,10] By adopting extended tetrathiafulvalene (TTF) dithiolene ligands, Kobayashi's group was able to determine the first crystal

* To whom correspondence should be addressed. E-mail: llusar@qfa.uji.es (R.L.); barrera@sg.uji.es (C.V.).
† Departament de Química Física y Analítica, Universitat Jaume I.
‡ Serveis Centrals d'Instrumentació Cientifica, Universitat Jaume I.
§ Instituto de Ciencia Molecular, Universitat de Valencia.
|| Sciences Chimiques de Rennes, Université Rennes 1.

(1) Coomber, A. T.; Beljonne, D.; Friend, R. H.; Bredas, J. L.; Charlton, A.; Robertson, N.; Underhill, A. E.; Kurmoo, M.; Day, P. *Nature* **1996**, *380*, 144.
(2) Faulmann, C.; Cassoux, P. *Prog. Inorg. Chem.* **2003**, *52*, 399.
(3) Cassoux, P.; Valade, L.; Kobayashi, H.; Kobayashi, A.; Clark, R. A.; Underhill, A. E. *Coord. Chem. Rev.* **1991**, *110*, 115.
(4) Pullen, A. E.; Olk, R.-M. *Coord. Chem. Rev.* **1999**, *188*, 211–262.
(5) Matsubayashi, G.; Nakano, M.; Tamura, H. *Coord. Chem. Rev.* **2002**, *226*, 143.
(6) Kato, R. *Chem. Rev.* **2004**, *104*, 5319.
(7) Kisch, H. *Coord. Chem. Rev.* **1993**, *125*, 155.
(8) Cummings, S. D.; Eisenberg, R. *Prog. Inorg. Chem.* **2003**, *52*, 315.
(9) Canadell, E. *New J. Chem.* **1997**, *21*, 1147.
(10) Canadell, E. *Coord. Chem. Rev.* **1999**, *629*, 185–186.

10.1021/ic8009546 CCC: $40.75
Published on Web 09/23/2008

structure of a metallic crystal based on neutral molecules, namely, $Ni(tmdt)_2$ (tmdt = trimethylenetetrathiafulvalenedithiolate), with a stable metallic state down 0.6 K and a room temperature conductivity of ~400 S cm^{-1}.[11]

In compound $Ni(tmdt)_2$, in addition to the generation of radicals in the neutral molecules, the existence of conduction paths was associated to (i) a small energetic separation between the HOMO−LUMO orbitals and (ii) the formation of extended 3-D networks through transversal S···S contacts involving sulfur π-orbitals.[12−14] On the basis of these guideline principles, new single-component molecular conductors have been prepared by tailored-design of molecules with small HOMO−LUMO gap (i), and in this context, the use of transition metal complexes with dithiolene ligands having a TTF skeleton has been preferred.[15−21] However, control of the crystal ordering that will actually determine the intermolecular contacts in the extended solid (ii) and, hence, its collective properties is more difficult to anticipate, and single-component molecular conductors with semiconducting or metallic properties can be obtained. A major challenge that remains is the solid-state characterization of these single-component conductors because of the inherent low solubility of these neutral complexes, and in some cases, this limitation has hindered a detailed understanding of innate electronic features of neutral dithiolene solid state architectures.[22−26]

The progress in the field of single-component molecular conductors is currently focused on the coordination of extended TTF dithiolene ligands to transition metals in a desire to vary and optimize the electronic properties of the resulting complexes. In this sense, replacement of the transition metal by more complex polynuclear entities represents a very attractive and promising approach. Some published examples include dinuclear rhenium compounds,[27] halide-bridged dinuclear $Ni_2(\mu$-Cl) units,[28] trinuclear Mo_3S_7 complexes,[29] or tetranuclear copper clusters.[26] These polynuclear entities might confer new electronic features associated to the tuneable relative energy of the cluster core and the dithiolene ligand, which might become available for extensive mixing leading to sizable electronic delocalization around the metallic core and the dithiolene ligand. In the case of mononuclear $M(dithiolene)_2$ transition metal complexes, metal−ligand orbital mixing depends on the position of the metal atom in the periodic table, its effective nuclear charge, and relativistic effects.[30]

Scheme 1

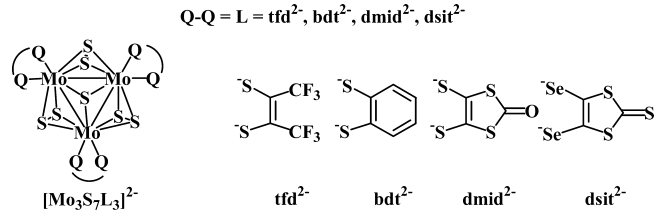

Recently, we have explored the possibility of replacing the transition metal in these mononuclear complexes by the group 6 trinuclear cluster unit of formula $[Mo_3(\mu_3\text{-}S)(\mu\text{-}S_2)_3]^{4+}$. The metal atoms in this cluster core define an equilateral triangle capped by one μ_3-S sulfur atom and with the molybdenum atoms bridged by disulfide ligands. This arrangement results in idealized C_{3v} symmetry for the cluster core. Chemical or electrochemical oxidation of the trinuclear $[Mo_3S_7(dmit)_3]^{2-}$ dianion (dmit = (1,3-dithia-2-thione-4,5-dithiolate) provides a neutral paramagnetic $Mo_3S_7(dmit)_3$ species, which is semiconducting in the solid state with a small activation energy (11−22 meV).[29] These results prompt us to develop analogous Mo_3S_7 complexes of general formula $[Mo_3S_7(dithiolene)_3]^{2-}$ and their oxidized $Mo_3S_7(dithiolene)_3$ counterparts with different dithiolate or diselenolate ligands aimed to evaluate the influence of the peripheral dithiolate (or diselenolate) ligands on the electronic and the solid-state structures of the cluster complex and on its collective (magnetic and transport) properties.

In this paper, we report the high yield synthesis, electrochemical characterization and solid-state structure of a series of $[Mo_3S_7(dithiolene)_3]^{2-}$ complexes with dithiolene = bis-(trifluoromethyl)-1,2-dithiolate ($\mathbf{4}^{2-}$), 1,2-benzenedithiolate ($\mathbf{5}^{2-}$), 1,3-dithiole-2-one-4,5-dithiolate ($\mathbf{6}^{2-}$), and $[Mo_3S_7(dsit)_3]^{2-}$ ($[\mathbf{7}]^{2-}$) (dsit =1,3-dithiole-2-thione-4,5-diselenolate). A simplified representation of the structure of these anionic clusters together with that of the dithiolate ligands is shown in Scheme 1. DFT calculations have been carried

(11) Tanaka, H.; Okano, Y.; Kobayashi, H.; Suzuki, W.; Kobayashi, A. *Science* **2001**, *291*, 285.
(12) Rovira, C.; Novoa, J. J.; Mozos, J. L.; Ordejón, P.; Canadell, E. *Phys. Rev. B* **2002**, *65*, 081104.
(13) Kobayashi, A.; Suzuki, W.; Fujiwara, E.; Otsuka, T.; Tanaka, H.; Okano, Y.; Kobayashi, H. *Mol. Cryst. Liq. Cryst.* **2002**, *379*, 19.
(14) Kobayashi, A.; Zhou, B.; Kobayashi, H. *J. Mater. Chem.* **2005**, *15*, 2078.
(15) Dautel, O. J.; Fourmigue, M.; Canadell, E.; Auban-Senzier, P. *Adv. Funct. Mater.* **2002**, *12*, 693.
(16) Tanaka, H.; Kobayashi, H.; Kobayashi, A. *J. Am. Chem. Soc.* **2002**, *124*, 10002.
(17) Suzuki, W.; Fujiwara, E.; Kobayashi, A.; Fujishiro, Y.; Nishibori, E.; Takata, M.; Sakata, M.; Fujiwara, H.; Kobayashi, H. *J. Am. Chem. Soc.* **2003**, *125*, 1486.
(18) Kobayashi, A.; Fujiwara, E.; Kobayashi, H. *Chem. Rev.* **2004**, *104*, 5243.
(19) Sasa, M.; Fujiwara, E.; Kobayashi, A.; Ishibashi, S.; Terakura, K.; Okano, Y.; Fujiwara, H.; Kobayashi, H. *J. Mater. Chem.* **2005**, *15*, 155.
(20) Zhou, B.; Shimamura, M.; Fujiwara, E.; Kobayashi, A.; Higashi, T.; Nishibori, E.; Sakata, M.; Cui, H.; Takahashi, K.; Kobayashi, H. *J. Am. Chem. Soc.* **2006**, *128*, 3872.
(21) Wen, H. R.; Li, C. H.; Zu, J. L.; Zhang, B.; You, X. Z. *Inorg. Chem.* **2007**, *46*, 6837.
(22) Belo, D.; Alves, H.; Lopes, E. B.; Duarte, M. B.; Gama, V.; Henriques, R. T.; Almeida, M.; Pérez-Benitez, A.; Rovira, C.; Veciana, J. *Chem.—Eur. J.* **2001**, *7*, 511.
(23) Kubo, K.; Nakano, M.; Hamaguchi, M.; Matsubayashi, G. *Inorg. Chim. Acta* **2003**, *346*, 43.
(24) Ryowa, T.; Nakano, M.; Tamura, H.; Matsubayashi, G. *Inorg. Chim. Acta* **2004**, *357*, 3532.
(25) Fujiwara, E.; Kobayashi, A.; Fujiwara, H.; Kobayashi, H. *Inorg. Chem.* **2004**, *43*, 1122.
(26) Belo, D.; Figueira, M. J.; Mendonça, J.; Santos, I. C.; Almeida, M.; Henriques, R. T.; Duarte, M. B.; Rovira, C.; Veciana, J. *Eur. J. Inorg. Chem.* **2005**, 3337.
(27) Matsubayashi, G.; Maikawa, T.; Tamura, H.; Nakano, M.; Arakawa, R. *J. Chem. Soc., Dalton Trans.* **1996**, 1539.
(28) Liu, S. X.; Ambrus, C.; Dolder, S.; Neels, A.; Decurtins, S. *Inorg. Chem.* **2006**, *45*, 9622.
(29) Llusar, R.; Uriel, S.; Vicent, C.; Coronado, E.; Gomez-Garcia, C. J.; Clemente-Juan, J. M.; Braida, B.; Canadell, E. *J. Am. Chem. Soc.* **2004**, *126*, 12076.
(30) Ray, K.; Petrenko, T.; Wieghardt, K.; Neese, F. *Dalton Trans.* **2007**, 1552.

out to evaluate the electronic structure of these clusters, in particular, the contribution from the Mo_3S_7 cluster core and the different dithiolene ligands to the valence molecular orbitals in the dianionic $\mathbf{4}^{2-}$ to $\mathbf{7}^{2-}$ compounds. Upon oxidation, dianionic $\mathbf{6}^{2-}$ and $\mathbf{7}^{2-}$ cluster complexes afford neutral paramagnetic species as microcrystalline powders. The intrinsic characteristics of these molecules fulfill the requirements needed to obtain magnetic single component molecular conductors, and as a consequence, their magnetic and transport properties have been investigated.

Experimental Section

Physical Measurements. IR spectra were recorded in the 300−3500 cm^{-1} range on a Perkin-Elmer System 2000 FT-IR using KBr pellets. Characteristic IR frequencies for the tfd, bdt, dmid, and dsit ligands, as well as the Mo_3S_7 cluster core were assigned on the basis of previously reported complexes.[31−34] XPD were obtained on a SIEMENS D5000 diffractometer using Cu Kα radiation. Electronic spectra (300−900 nm) were recorded on KBr pellets with a VARIAN UV−vis spectrophotometer (model CARY 500 SCAN) equipped with a diffuse reflectance accessory. ^{1}H NMR spectra were recorded on Varian Unity Inova-500 spectrometer, using $CDCl_3$, and are referenced to internal tetramehtylsilane. A Quattro LC (quadrupole-hexapole-quadrupole) mass spectrometer with an orthogonal Z-spray electrospray interface (Waters, Manchester, UK) was used. The chemical composition of each peak in the scan mode was assigned by comparison of the isotope experimental pattern with that calculated using the MassLynx 4.0 program. Cyclic voltammetry experiments were performed with a Echochemie Pgstat 20 electrochemical analyzer. All measurements were carried out with a conventional three-electrode configuration consisting of platinum working and auxiliary electrodes and a Ag/AgCl reference electrode containing aqueous 3 M KCl. The solvent used in all experiments was CH_2Cl_2 (Merck HPLC grade), which was deoxygenated before use. The supporting electrolyte was 0.1 M tetrabutylammonium hexafluorophosphate. $E_{1/2}$ values were determined as $1/2(E_a + E_c)$, where E_a and E_c are the anodic and cathodic peak potentials, respectively. DC. conductivity measurements over the range of 2−300 K were performed on pressed pellets with a Quantum Design PPMS-9 model. Magnetic measurements were done on a polycrystalline sample with a commercial SQUID susceptometer (Quantum Design MPMS-XL-5) in the temperature range of 2−300 K with an applied magnetic field of 0.05 T. The sample susceptibility was corrected for the sample holder contribution, previously measured in the same conditions, and for the diamagnetic contribution of the constituent atoms (Pascal's tables).

General Procedures. All reactions were carried under inert atmosphere unless otherwise stated. The compounds $(n\text{-Bu})_2$Sn(dmid), $(n\text{-Bu}_4\text{N})_2[Mo_3S_7Br_6]$, and $(n\text{-Bu}_4\text{N})_2[Zn(dsit)_2]$ were prepared according to literature methods.[35−37] The remaining reactants were obtained from commercial sources and were used as received. Solvents for synthesis were dried and degassed by standard methods before use.

Preparation of $(n\text{-Bu})_2$Sn(bdt) (1). Et_3N (160 μL, 1.1 mmol) was added to a solution of 1,2-benzenedithiol (60 μL, 0.5 mmol) in 20 mL of THF, and the resulting solution was stirred for two hours. After the mixture was cooled to −78 °C, a solution of $(n\text{-Bu}_4)_2SnCl_2$ (0.15 g, 0.5 mmol) in THF (10 mL) was added dropwise for 1 h, and the reaction mixture was allowed to warm to 0 °C. The reaction was quenched by the addition of water, and the resulting mixture was extracted with three portions of chloroform. The extracts were combined, dried over $MgSO_4$, then evaporated under reduced pressure to yield compound **1** as a yellow oil (0.17 g, 88%). ^{1}H NMR ($CDCl_3$): δ 0.93 (t, 6 H), 1.40 (m, 4 H), 1.67 (t, 4 H), 1.75 (m, 4 H), 6.89 (dd, 2H), 7.46 (dd, 2H). ESI-MS(−) *m*/*z*: 409 $[M + Cl]^-$.

Preparation of $(n\text{-Bu})_2$Sn(tfd) (2). 4,5-Bis(trifluoromethyl)-1,3-dithiole-2-one,[38] (1 g, 3.93 mmol) was treated with ^{t}BuOK (1.01 g, 9 mmol) in dry THF (50 mL). After the mixture was stirred for 1 h, Bu_2SnCl_2 (1.43 g, 4.7 mmol) dissolved in THF (5 mL) was added dropwise to the suspension, and the orange solution was stirred for 2.5 h. Evaporation of the solvent and column chromatography (silica gel, eluant CH_2Cl_2) afforded an orange oil. Slow evaporation under N_2 of a hexane solution afforded colorless crystals (1.4 g, 77%). ^{1}H NMR ($CDCl_3$): δ 0.93 (t, 6 H), 1.39 (m, 4 H), 1.60 (t, 4 H), 1.74 (m, 4 H). ESI-MS(−) *m*/*z*: 495 $[M + Cl]^-$.

Preparation of $(n\text{-Bu})_2$Sn(dsit) (3). Lithium diisopropylamide (0.85 g, 8 mmol) was added to a solution of vinylentrithiocarbonate (0.54 g, 4 mmol) in 40 mL of dry THF, and the mixture was stirred during 2 h at the temperature of −78 °C. After that, Se powder (0.63 g, 8 mmol) was added, and the mixture was stirred for 1 h; the reaction mixture was allowed to warm to room temperature. After the mixture was cooled to −78 °C again, a solution of $(n\text{-Bu}_4)_2SnCl_2$ (1.36 g, 4.5 mmol) in THF (10 mL) was added dropwise for 1 h, and the reaction mixture was allowed to warm to 0 °C. The reaction was quenched by the addition of water, and the resulting mixture was extracted with three portions of chloroform. The extracts were combined, dried over $MgSO_4$, then evaporated under reduced pressure to yield compound **3** as a yellow oil (0.17 g, 88%). ^{1}H NMR ($CDCl_3$): δ 0.93 (t, 6 H), 1.40 (m, 4 H), 1.67 (t, 4 H), 1.75 (m, 4 H), 6.90 (m, 2H), 7.5 (m, 2H). ESI-MS(−) *m*/*z*: 559 $[M + Cl]^-$.

Preparation of $(n\text{-Bu}_4\text{N})_2[Mo_3S_7(tfd)_3]$ ($(n\text{-Bu}_4\text{N})_2$[4]). $(n\text{-Bu})_2$Sn(tfd) (0.14 g, 0.30 mmol) was added to an orange solution of $(n\text{-Bu}_4\text{N})_2[Mo_3S_7Br_6]$ (0.15 g, 0.10 mmol) in 15 mL of CH_3CN under nitrogen. An immediate color change was observed from orange to red. The solution was stirred under reflux conditions for 3 h, and the desired compound $(n\text{-Bu}_4\text{N})_2$[**4**] was precipitated with diethylether. The precipitate was separated from the solution by filtration and dried in vacuo (0.96 g, 57%). (Found: C, 31.74; H, 4.28; N, 1.58. $Mo_3S_{13}C_{48}H_{72}N_2F_{18}$ requires C, 33.45; H, 4.21; N, 1.63.) IR (KBr) cm^{-1}: 1440 (s, ν(C═C)); 552 (m, $\nu(S_{eq}-S_{ax})$): 449 (m, ν(Mo-(μ_3-S)); 358 (w, ν(Mo-(μ-S_{ax})); 335 (w, ν(Mo-(μ-S_{eq})). ESI-MS(−) *m*/*z*: 595 $[M]^{2-}$.

Preparation of $(n\text{-Bu}_4\text{N})_2[Mo_3S_7(bdt)_3]$ ($(n\text{-Bu}_4\text{N})_2$[5]). This compound was prepared following the procedure described for $(n\text{-Bu}_4\text{N})_2$[**4**] by using $(n\text{-Bu})_2$Sn(bdt) (0.11 g, 0.30 mmol) and $(n\text{-Bu}_4\text{N})_2[Mo_3S_7Br_6]$ (0.15 g, 0.10 mmol) to yield a microcrystalline red powder. (0.12 g, 89%). (Found: C, 41.45; H, 5.88; S, 29.10; N, 1.96. $Mo_3S_{13}C_{50}H_{84}N_2$ requires C, 42.35; H, 5.97; S, 29.40; N,

(31) Wang, K.; McConnachie, J. M.; Stiefel, E. I. *Inorg. Chem.* **1999**, *38*, 4334.
(32) Llusar, R.; Triguero, S.; Vicent, C.; Sokolov, M. N.; Domercq, D.; Fourmigue, M. *Inorg. Chem.* **2005**, *44*, 8937.
(33) Olk, R. M.; Rohr, A.; Sieler, J.; Kohler, K.; Kirsme, R.; Dietzsch, W.; Hoyer, E.; Olk, B. *Z. Anorg. Allg. Chem.* **1989**, *577*, 206.
(34) Fedin, V. P.; Kolesov, B. A.; Mironov, Y. V.; Fedorov, V. Y. *Polyhedron* **1989**, *8*, 2419.
(35) Yamada, J. I. *J. Org. Chem.* **1996**, *61*, 3987.
(36) Fedin, V. P.; Sokolov, M. N.; Mironov, Y. V.; Kolesov, B. A.; Tkachev, S. V.; Fedorov, V. Y. *Inorg. Chim. Acta* **1990**, *167*, 39.
(37) Poleschner, H.; Radeglia, R.; Fuchs, J. *J. Organomet. Chem.* **1992**, *427*, 213.
(38) Jeannin, O.; Fourmigue, M. *Chem.—Eur. J.* **2006**, *12*, 2994.

Table 1. Crystallographic Data for $(n\text{-}Bu_4N)_2[Mo_3S_7(bdt)_3]$ $(n\text{-}Bu_4N)_2$**[5]**, $(n\text{-}Bu_4N)_2[Mo_3S_7(dmid)_3]\cdot C_4H_{10}O$ $(n\text{-}Bu_4N)_2$**[6]**$\cdot C_4H_{10}O$, and $(n\text{-}Bu_4N)_2[Mo_3S_7(dsit)_3]\cdot {}^1/_2CH_2Cl_2$ $(n\text{-}Bu_4N)_2$**[7]**$\cdot {}^1/_2CH_2Cl_2$

compound	$(n\text{-}Bu_4N)_2$**[5]**	$(n\text{-}Bu_4N)_2$**[6]**$\cdot C_4H_{10}O$	$(n\text{-}Bu_4N)_2$**[7]**$\cdot {}^1/_2CH_2Cl_2$
empirical formula	$C_{50}H_{84}Mo_3N_2S_{13}$	$C_{61}H_{50}Mo_3O_4P_2S_{19}$	$C_{41.50}H_{73}ClMo_3N_2S_{16}Se_6$
fw	1417.79	1805.91	1910.01
cryst syst	monoclinic	triclinic	monoclinic
a, Å	16.6096(9)	15.490(3)	16.366(9)
b, Å	23.6618(13)	15.639(3)	25.154(14)
c, Å	17.7170(10)	17.050(3)	18.158(11)
α, deg		76.244(5)	
β, deg	110.057(1)	65.066(4)	107.677(16)
γ, deg		89.185(5)	
V, Å^3	6540.7(6)	3620.5(12)	7122(7)
T, K	293(2)	293(2)	293(2)
space group	P2(1)/c	P−1	P2(1)/n
Z	4	2	4
μ(Mo Kα), mm^{-1}	1.014	1.149	4.123
reflns collected	44 198	20 610	31 344
ϕ range for data collection	1.31−27.50	1.35−25.00	1.54−22.50
unique reflns/R_{int}	14 952 [R_{int} = 0.0700]	12 706 [R_{int} = 0.0808]	9272 [R_{int} = 0.0994]
GOF on F^2	1.074	1.071	1.023
R1[a]/wR2[b]	R1 = 0.0543, wR2 = 0.1352	R1 = 0.0839, wR2 = 0.1853	R1 = 0.0613, wR2 = 0.1538
R1[a]/wR2[b] (all data)	R1 = 0.1239, wR2 = 0.1817	R1 = 0.2107, wR2 = 0.2397	R1 = 0.1228, wR2 = 0.1884
residual ρ, e A^{-3}	0.881 and −0.654	1.297 and −1.145	1.014 and −0.658

[a] $R1 = \sum||F_o|-|F_c||/\sum F_o$. [b] $wR2 = [\sum[w(F_o^2 - F_c^2)^2]/\sum[w(F_o^2)^2]]^{1/2}$.

1.98.) IR (KBr) cm^{-1}: 1440 (s, ν(C═C)); 552 (m, $\nu(S_{eq}-S_{ax})$); 449 (m, ν(Mo−(μ_3-S)); 358 and 339 (w) ν(Mo−(μ-S_{ax})), ν(Mo−(μ-S_{eq})). ESI-MS(−) *m*/*z*: 467 $[M]^{2-}$.

Preparation of $(n\text{-}Bu_4N)_2[Mo_3S_7(dmid)_3]$ ($(n\text{-}Bu_4N)_2$[6]). This compound was prepared following the procedure described for $(n\text{-}Bu_4N)_2$**[4]** by using $(n\text{-}Bu)_2Sn(dmid)$ (0.20 g, 0.48 mmol) and $(n\text{-}Bu_4N)_2[Mo_3S_7Br_6]$ (0.15 g, 0.10 mmol) to yield a microcrystalline violet powder (0.21 g, 85%). (Found: C, 32.47; H, 4.65; S, 39.56; N, 1.86. $Mo_3S_{19}C_{41}H_{72}N_2O_3$ requires C, 32.02; H, 4.72; S, 39.61; N, 1.82). IR (KBr) cm^{-1}: 1663 (s, ν(C═O)); 1611 (s, ν(C═O)), 1481 (s, ν(C═C)); 893 (m, ν(C−S)); 552 (m, $\nu(S_{eq}-S_{ax})$); 449 (m, ν(Mo−(μ_3-S)); 358 (w) and 335 (w) ν(Mo−(μ-S_{ax}), ν(Mo−(μ-S_{eq})). ESI-MS(−) *m*/*z*: 527 $[M]^{2-}$.

Preparation of $(n\text{-}Bu_4N)_2[Mo_3S_7(dsit)_3]$ ($(n\text{-}Bu_4N)_2$[7]). This compound was prepared following the procedure described for $(n\text{-}Bu_4N)_2$**[4]** by using $(n\text{-}Bu_4N)_2[Zn(dsit)_2]$ (0.17 g, 0.15 mmol) and $(n\text{-}Bu_4N)_2[Mo_3S_7Br_6]$ (0.15 g, 0.10 mmol) to yield a microcrystalline violet powder. (0.05 g, 58%). (Found: C, 25.89; H, 3.85; N, 1.47; S, 27.42. $Mo_3S_{16}C_{41}H_{72}N_2$ requires C, 26.37; H, 3.88; N, 1.50; S, 27.47.). IR (KBr) cm^{-1}: 1456 (s, ν(C═C)); 1050 (m, ν(C═S)); 530 (m, $\nu(S_{eq}-S_{ax})$); 463 (w, ν(Mo−(μ_3-S)), 359 (w) and 338 (w) ν(Mo−(μ-S_{ax})), ν(Mo−(μ-S_{eq})). ESI-MS(−) *m*/*z*: 692 $[M]^{2-}$.

Preparation of $Mo_3S_7(dmid)_3$ (6). A solution of iodine (0.101 g, 0.40 mmol) in acetone (10 mL) was layered to dichloromethane solutions of $(n\text{-}Bu_4N)_2$**[4]** (0.15 g, 0.10 mmol). The resulting dark precipitate was separated by centrifugation, washed thoroughly with dichloromethane and dried in vacuo to yield a microcrystalline black powder (0.06 g, 67%). (Found: C, 10.86; S, 55.61. $Mo_3S_{19}C_9O_3$ requires C, 10.26; S, 57.85.) IR (KBr) cm^{-1}: 1678 (s, ν(C═O)); 1609 (s, ν(C═O)); 1284 (s, ν(C═C)); 537 (m, $\nu(S_{eq}-S_{ax})$); 468 and 336 (w) ν(Mo−(μ-S_{ax}), ν(Mo−(μ-S_{eq})).

Preparation of $Mo_3S_7(dsit)_3$ (7). This compound was prepared following the procedure described for **6** by using iodine (0.101 g, 0.40 mmol) and $(n\text{-}Bu_4N)_2$**[7]** (0.19 g, 0.10 mmol) to yield a microcrystalline black powder (0.06 g, 47%). (Found: C, 8.15; S, 37.22. $Mo_3S_{16}Se_6C_9$ requires C, 7.82; S, 37.10.) IR (KBr) cm^{-1}: 1463 (s) ν(C═C); 1027 (s) ν(C═S); 562 (m, $\nu(S_{eq}-S_{ax})$); 452 and 343 (w) ν(Mo−(μ-S_{ax})), ν(Mo−(μ-S_{eq})).

Structural Determination. Crystals of compound $(n\text{-}Bu_4N)_2$**[5]** and $(n\text{-}Bu_4N)_2$**[7]** suitable for X-ray studies were grown by slow diffusion of diethylether onto CH_2Cl_2 solutions. Crystals for X-ray studies of the tetraphenylphosphonium salt, $(PPh_4)_2$**[6]**$\cdot C_4H_{10}O$ were obtained by addition of an excess of $(PPh_4)Br$ to a CH_2Cl_2 solution of $(n\text{-}Bu_4N)_2$**[6]** and further recrystallization from CH_2Cl_2/diethylether. The X-ray diffraction experiment was carried out on a Bruker SMART CCD diffractometer using Mo Kα radiation (λ = 0.71073 Å) at room temperature. The data were collected with a frame width of 0.3 in $\bar{\omega}$ at a crystal-to-detector distance of 4 cm. The diffraction frames were integrated using the SAINT package and corrected for absorption with SADABS.[39,40] The structure was solved by direct methods and refined by the full-matrix method based on F^2 using the SHELXTL software package.[41] The crystal parameters and basic information relating data collection and structure refinement are summarized in Table 1.

In compound $(n\text{-}Bu_4N)_2$**[5]**, all cluster and tetrabutylammonium cations were refined anisotropically. The bond distances of the carbon atoms C(113)−C(114), C(114)−C(115), and C(202)−C(203) were constrained at fixed value. Hydrogen atoms of the phenyl groups were introduced at calculated positions with a riding model. In compound $(PPh_4)_2$**[6]**$\cdot C_4H_{10}O$, all cluster atoms were refined anisotropically. Two $[PPh_4]^+$ cations were found and the phosphorus atoms were refined anisotropically. Carbon atoms on the cation centered at P(10) were refined anisotropically, and hydrogen atoms were generated geometrically. Carbon atoms on the second cation centered at P(20) were refined isotropically. One phenyl group on the second cation appeared disordered in two nearby positions and was refined as a rigid group with half-occupancies over the two positions. One diethylether molecule was found in the last Fourier maps and was refined isotropically under rigid conditions. In compound $(n\text{-}Bu_4N)_2$**[7]**, all cluster atoms were refined anisotropically. Two $[n\text{-}Bu_4N]^+$ cations were found, and the nitrogen atoms were refined anisotropically whereas carbon atoms were refined isotropically. The bond distance of the carbon atoms C(109)−C(110) in the cation centered at N(100) was constrained at fixed value. The $[n\text{-}Bu_4N]^+$ cation centered at N(200) was refined as rigid group. Hydrogen atoms of the buthyl groups were introduced at calculated

(39) *SAINT*, version 5.0; Bruker Analytical X-Ray Systems: Madison, WI, 1996.
(40) G. M., Sheldrick. *SADABS, Empirical Absorption Program*; University of Göttingen: Göttingen, Germany, 1996.
(41) G. M., Sheldrick. *SHELXTL*, version 5.1; Bruker Analytical X-Ray Systems: Madison, WI, 1997.

positions with a riding model. Half a molecule of CH_2Cl_2 was found in the last Fourier maps and was refined anisotropically.

Computational Details. All calculations were carried out using the ADF 2005 program.[42] All species studied were optimized starting from the X-ray structural parameters using DFT calculations, in particular the BP86 generalized gradient approximation,[43,44] triple-ν plus polarization Slater-type orbital basis sets, (BP86/VTZP) and a fine mesh for numerical integration of the matrix elements. Large frozen cores (Mo.4p, Se.3p, S.2p, F.1s, O.1s, C.1s) were employed. Relativistic effects are considered using the ZORA formalism.[45−47]

Results and Discussion

Synthesis, Crystal Structure, and Electrochemistry of Mo_3S_7 Dianionic Clusters. General synthetic procedures for dithiolene coordination essentially relies on the use of bis-thioesther compounds in the presence of strong bases with metal halides, followed by precipitation with tatralkylammonium salts.[4,48] By using this approach, the synthesis of their polynuclear counterparts remains less rationalized mainly because of the limited stability of the polynuclear entities in the presence of strong bases and the tendency of the dithiolene ligands to coordinate in several and often unexpected fashions. Regarding the family of Mo_3S_7 clusters, the $[Mo_3S_7Br_6]^{2-}$ dianion represents the most convenient starting material for dithiolene coordination. In this case, the use of "in situ" generated dithiolate alkaline salts leads to the partial degradation of the cluster core, thus resulting in tedious purification and low overall yields. Ligand substitution on the $[Mo_3S_7Br_6]^{2-}$ dianion using $(n\text{-}Bu_4N)_2$[Zn(dithiolate)] (dithiolate = dmit, tdas) or the Na_2(mnt) sodium salt circumvents such limitation and usually yields the desired dithiolene Mo_3S_7 complexes in moderate yields.[29,49,50] The workup procedure requires thoroughly washing to remove the excess of inorganic salts formed during the course of the reaction (ZnBr or NaBr) and further recrystallization to obtain the desired compounds in analytically pure form. In the present work, we have sought a direct and reasonably general method for preparing 1,2-bisdithiolene Mo_3S_7 complexes. The procedure is based on the use of dithiolene tin complexes of general formula $(n\text{-}Bu)_2$Sn(dithiolate) according to reaction 1. Such tin derivatives have already proven to be very efficient dithiolate transfer agents for the preparation of monometallic dithiolene complexes, affording much cleaner reactions with formation of neutral byproduct, such as $(n\text{-}Bu)_2SnBr_2$.[51−54]

$$(n\text{-}Bu_4N)_2[Mo_3S_7Br_6] + 3(Bu)_2Sn(\text{dithiolate}) \rightarrow (n\text{-}Bu_4N)_2[Mo_3S_7(\text{dithiolate})_3] + 3(Bu)_2SnBr_2 \quad (1)$$

Treatment of $(n\text{-}Bu_4N)_2[Mo_3S_7Br_6]$ with an excess of the corresponding $(Bu)_2$Sn(dithiolate) complex affords the ligand substitution products $(n\text{-}Bu_4N)_2$[**4**]−$(n\text{-}Bu_4N)_2$[**6**], which are readily separated from the putative $(Bu)_2SnBr_2$ species and the excess of $(Bu)_2$Sn(dithiolate) by simple precipitation with diethylether. This route is applicable to different dithiolene ligands (bdt, tfd and dmid) with different substituent effects to afford compounds $(n\text{-}Bu_4N)_2$[**4**]−$(n\text{-}Bu_4N)_2$[**6**] in moderate to high yield. The main advantages of this route rely on the easy availability of the tin complexes for a wide spectrum of dithiolene ligands and the simplified purification step to isolate the desired Mo_3S_7 cluster complexes. In the case of the 1,3-dithia-2-thione-4,5-diselenolate (dsit) ligand, the use of the $(n\text{-}Bu_4)_2$Sn(dsit) does not lead to ligand coordination to the Mo_3S_7 core, presumably, because of the inactive Sn−Se bonds. The zinc salt, namely, $(n\text{-}Bu_4N)_2[Zn(dsit)_2]$ was required to obtain compound $(n\text{-}Bu_4N)_2$[**7**] in 58% yield.

Compounds $(n\text{-}Bu_4N)_2$[**4**]-$(n\text{-}Bu_4N)_2$[**7**] have been characterized by electrospray ionization mass spectrometry revealing in all cases the presence of intact M^{2-} dianions as base peak. Compounds $(n\text{-}Bu_4N)_2$[**5**], $(PPh_4)_2$[**6**], and $(n\text{-}Bu_4N)_2$[**7**] have also been characterized X-ray single-crystal analysis. The main geometric features of the Mo_3S_7 cluster core are similar for compounds $(n\text{-}Bu_4N)_2$[**5**]-$(n\text{-}Bu_4N)_2$[**7**]. An ORTEP representation for the $\mathbf{5}^{2-}$ and $\mathbf{7}^{2-}$ dianions is exemplified in Figure 1.

The molecular structure of $\mathbf{5}^{2-}$, $\mathbf{6}^{2-}$, and $\mathbf{7}^{2-}$ reveals the presence of an equilateral Mo_3 core capped by a μ_3-S^{2-} atom that lies above the metallic plane. In addition, three bridging μ-S_2^{2-} groups connect adjacent metal atoms with three sulfur atoms occupying an equatorial position (S_{eq}, those labeled as S(3), S(5), and S(7)) essentially in the Mo_3 plane and three axial sulfur atoms (S_{ax}, those labeled as S(2), S(4) and S(6)) located out of the metal plane. The dithiolate or diselenolate groups fill the remaining two positions on the seven-coordinated molybdenum atoms and are oriented almost perpendicular to the Mo_3 plane. Table 2 collects the most relevant bond distances for these compounds together with those calculated for the optimized structures; we will refer to these last values later on in this discussion.

A common structural feature of Mo_3S_7 clusters is related to the prominent electrophilic character of the three axial sulfur atoms. As a consequence, the pocket defined by these axial sulfur atoms is typically occupied by different isolated mono- or dianions[55−57] leading to diverse solid-state Mo_3S_7

(42) Velde, G. T.; Bickelhaupt, F. M.; Baerends, E. J.; Guerra, C. F.; Van Gisbergen, S. J. A.; Snijders, J. G.; Ziegler, T. *J. Comput. Chem.* **2001**, *22*, 931.
(43) Becke, A. D. *J. Chem. Phys.* **1986**, *84*, 4524.
(44) Perdew, J. P.; Yue, W. *Phys. Rev. B* **1986**, *33*, 8800.
(45) Vanlenthe, E.; Baerends, E. J.; Snijders, J. G. *J. Chem. Phys.* **1993**, *99*, 4597.
(46) Vanlenthe, E.; Baerends, E. J.; Snijders, J. G. *J. Chem. Phys.* **1994**, *101*, 9783.
(47) Vanlenthe, E.; Snijders, J. G.; Baerends, E. J. *J. Chem. Phys.* **1996**, *105*, 6505.
(48) Cassoux, P. *Coord. Chem. Rev.* **1999**, *186*, 213.
(49) Garriga, J. M.; Llusar, R.; Uriel, S.; Vicent, C.; Usher, A. J.; Lucas, N. T.; Humphrey, M. G.; Samoc, M. *Dalton Trans.* **2003**, 4546.
(50) Alberola, A.; Llusar, R.; Triguero, S.; Vicent, C.; Sokolov, M. N.; Gómez-Garcia, C. *J. Mater. Chem.* **2007**, *17*, 3440.
(51) Velazquez, C. S.; Baumann, T. F.; Olmstead, M. M.; Hope, H.; Barrett, A. G. M.; Hoffman, B. M. *J. Am. Chem. Soc.* **1993**, *115*, 9997.
(52) Cerrada, E.; Fernandez, E. J.; Jones, P. G.; Laguna, A.; Laguna, M.; Terroba, R. *Organometallics* **1995**, *14*, 5537.
(53) Cerrada, E.; Laguna, M.; Sorolla, P. A. *Polyhedron* **1997**, *17*, 295.
(54) Nomura, M.; Fourmigue, M. *Inorg. Chem.* **2008**, *47*, 1301.
(55) Zimmerman, H.; Hegetschweiler, K.; Keller, T.; Gramlich, V.; Schmalle, H.; Petter, W.; Schneider, W. *Inorg. Chem.* **1991**, *30*, 4336.

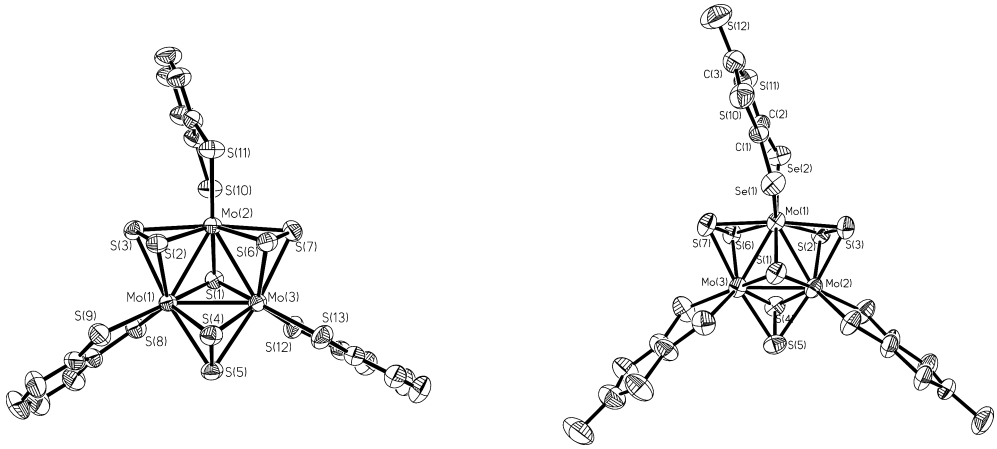

Figure 1. ORTEP representation (50% ellipsoids probability) for the $\mathbf{5}^{2-}$ (left) and the $\mathbf{7}^{2-}$ dianion (right).

Table 2. Selected Experimental and Theoretically Calculated Bond Distances for Compounds $\mathbf{4}^{2-}$ to $\mathbf{7}^{2-}$

	$[Mo_3S_7(tfd)_3]^{2-}$, $\mathbf{4}^{2-}$	$[Mo_3S_7(bdt)_3]^{2-}$, $\mathbf{5}^{2-}$		$[Mo_3S_7(dmid)_3]^{2-}$, $\mathbf{6}^{2-}$		$[Mo_3S_7(dsit)_3]^{2-}$, $\mathbf{7}^{2-}$	
distance (Å)	BP86/VTZP	BP86/VTZP	X-ray	BP86/VTZP	X-ray	BP86/VTZP	X-ray
Mo−Mo	2.855	2.856	2.786	2.850	2.777	2.815	2.761
Mo−(μ_3-S)	2.416	2.417	2.364	2.415	2.371	2.415	2.372
Mo−S_{eq}	2.578	2.573	2.521	2.572	2.514	2.555	2.511
Mo−S_{ax}	2.451	2.453	2.414	2.452	2.414	2.447	2.417
Mo−L_{trans} [a]	2.494	2.514	2.496	2.536	2.519	2.689	2.635
Mo−L_{cis} [b]	2.442	2.454	2.436	2.462	2.448	2.611	2.578
S_{ax}−S_{eq}	2.065	2.066	2.034	2.065	2.038	2.064	2.037

[a] L = S or Se atoms trans to Mo−(μ_3-S). [b] L = S or Se atoms cis to Mo−(μ_3-S).

arrangements.[58] The nature of this noncovalent interaction has been recently investigated using DFT calculations for the series of trianions $\{[Mo_3Q_7X_6]X\}^{3-}$ (Q = S, Se, Te; X = Cl, Br, I).[59] The identity of the outer ligands (such as halides or dithiolenes) also play a key structural directing role because of the potential formation of short contacts between sulfur atoms from neighboring clusters.[50,60] For the $\mathbf{5}^{2-}$, $\mathbf{6}^{2-}$, and $\mathbf{7}^{2-}$ dianions reported here, the crystal packing can be rationalized by considering the distinctive participation of the three axial sulfur atoms and the three outer dithiolene ligands in short contacts with neighboring clusters. Hence, the $\mathbf{5}^{2-}$, $\mathbf{6}^{2-}$, and $\mathbf{7}^{2-}$ dianions were all found to dimerize in the solid state through short S···S contacts (typically below 3.7 Å) between the three axial sulfur atoms and the S (or Se) atoms of one dithiolene ligand belonging to a neighbor cluster. These interactions, (illustrated in Figure 2a for the $\mathbf{5}^{2-}$ dianion) formally result in dimers of trimers in the solid state.

For the $\mathbf{5}^{2-}$ dianion lacking of heteroatoms in the dithiolene moiety, the remaining two dithiolate ligands are noninteracting, thus leading to discrete dimers. However, for complexes $(PPh_4)_2$[**6**] and $(n\text{-}Bu_4N)_2$[**7**], additional interactions between a second dmid or dsit ligand (that do not participate in the dimer formation with a neighbor cluster), give rise to the formation of infinite chains along the $[0\bar{1}1]$ and [101] directions, respectively through short contacts between crystallographically equivalent ligands. In both $(PPh_4)_2$[**6**] and $(n\text{-}Bu_4N)_2$[**7**] salts, a third dithiolene ligand appears noninteracting. As a result, the dithiolene or diselenolene ligands that participate in such interactions are slightly folded along the S−S or Se−Se hinge.

Cyclic voltammetry experiments of compounds $(n\text{-}Bu_4N)_2$[**4**]−$(n\text{-}Bu_4N)_2$[**7**] were performed in dichloromethane, and the redox potential values for the different processes observed are listed in Table 3. In all cases, the cyclic voltammograms are dominated by an irreversible reduction process in the −1.2 to −1.7 V range (versus Ag/AgCl). This process has also been observed for other Mo_3S_7 complexes at similar potentials and is ascribed to the reduction of three dichalcogenide ligands to afford the homologous sulfur-bridged complexes with an incomplete cuboidal Mo_3S_4 core.[49,50,55]

As previously reported, dithiolene coordination to the Mo_3S_7 core furnishes oxidation activity to the new complexes.[29,50] The number of observed oxidation processes, one or two, depends on the outer dithiolate or diselenolate ligand. For compounds $(n\text{-}Bu_4N)_2$[**4**] and $(n\text{-}Bu_4N)_2$[**5**], two successive reversible oxidations of equal intensity in the 0.0−0.9 V range are observed as previously found for the $(n\text{-}Bu_4N)_2[Mo_3S_7(mnt)_3]$ compound.[49] For the other two cluster salts, $(n\text{-}Bu_4N)_2$[**6**] and $(n\text{-}Bu_4N)_2$[**7**], only one oxidation process is registered in which asymmetry in the wave's shape is indicative of the deposition upon oxidation of conducting species at the electrode. This behavior was already observed for compound $(n\text{-}Bu_4N)_2[Mo_3S_7(dmit)_3]$ for which a two-electron oxidation process has been proposed based on the

(56) Mayor-Lopez, M. J.; Weber, J.; Hegetschweiler, K.; Meienberger, M. D.; Joho, F.; Leoni, S.; Nesper, R.; Reiss, G. J.; Frank, W.; Kolesov, B. A.; Fedin, V. P.; Fedorov, V. Y. *Inorg. Chem.* **1998**, *37*, 2633.
(57) Chen, J.; Lu, S. F.; Huang, Z. X.; Yu, R. M.; Wu, Q. J. *Chem.—Eur. J.* **2001**, *7*, 2002.
(58) Virovets, A. V.; Podberezskaya, N. V. *J. Struct. Chem.* **1993**, *34*, 305.
(59) Slepkov, V.; Kozlova, S.; Gabuda, S.; Fedorov, V. *J. Mol. Struct. TEOCHEM* **2008**, *849*, 112.
(60) Llusar, R.; Triguero, S.; Uriel, S.; Vicent, C.; Coronado, E.; Gomez-Garcia, C. J. *Inorg. Chem.* **2005**, *44*, 1563.

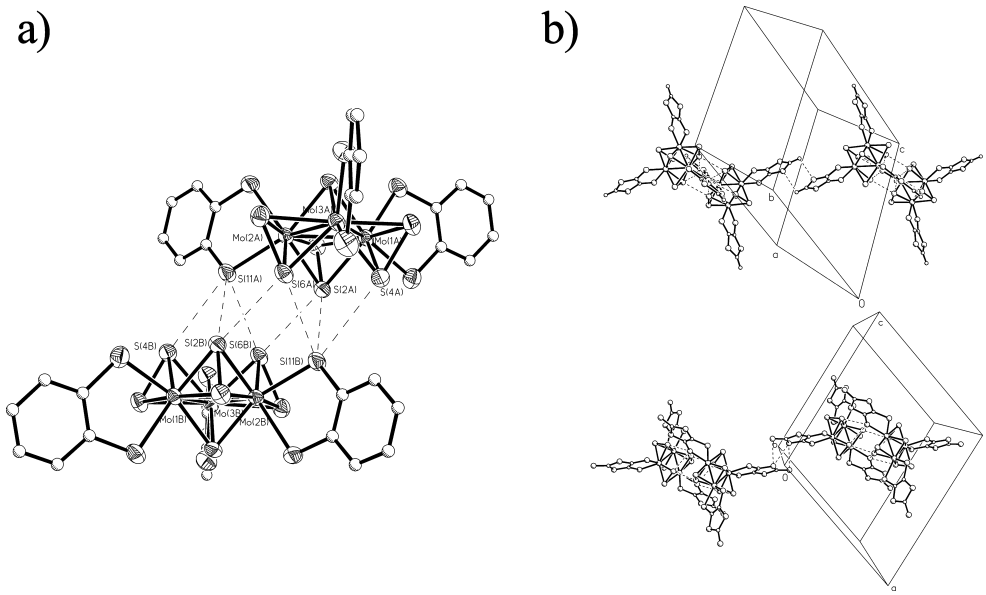

Figure 2. (a) Solid-state dimerization of dianion $\mathbf{5}^{2-}$ (also applicable to $\mathbf{6}^{2-}$ and $\mathbf{7}^{2-}$) and (b) packing diagram for compounds $(PPh_4)_2$[**6**] (top) and $(n\text{-}Bu_4N)_2$[**7**] (bottom), showing the cluster dimers and the S···S and S···O interactions between dimers.

Table 3. Redox Potentials[a] for the Tetrabuthylammonium Salts of Several Dithiolate and Diselenolate Mo_3S_7 Cluster Dianions in Dichloromethane

cluster dianion	reduction E_c[b](V)	oxidation $E_{1/2}$, ΔE[c] (V)	ref
$[Mo_3S_7(tfd)_3]^{2-}$, $\mathbf{4}^{2-}$	−1.22	0.51 (0.07), 0.89 (0.06)	this work
$[Mo_3S_7(bdt)_3]^{2-}$, $\mathbf{5}^{2-}$	−1.26	0.23 (0.07), 0.41 (0.13)	this work
$[Mo_3S_7(dmid)_3]^{2-}$, $\mathbf{6}^{2-}$	−1.27	0.36 (0.10 V)[d]	this work
$[Mo_3S_7(dsit)_3]^{2-}$, $\mathbf{7}^{2-}$	−1.69	0.34 (0.18 V)[d]	this work
$[Mo_3S_7(dmit)_3]^{2-}$	−1.20	0.38 (0.17 V)[d]	29
$[Mo_3S_7(tdas)_3]^{2-}$	−1.31	0.72 (0.076)	50
$[Mo_3S_7(mnt)_3]^{2-}$	−1.04	0.77 (0.071), 1.16(0.068)	49
$[Mo_3S_7Br_6]^{2-}$	−1.15		49

[a] $E_{1/2}$ (ferrocene/ferrocene+) = 0.44 V (ΔE 66 mV). [b] Potentials measured at 100 mV s^{-1}. [c] $\Delta E = |E_a - E_c|$. [d] Asymmetric wave.

isolation of neutral $Mo_3S_7(dmit)_3$ species.[29] The easiness toward oxidation within the $[Mo_3S_7L_3]^{2-}$ (L = bdt, tfd, mnt, tdas) series follows the trend bdt > tfd > tdas > mnt. In a similar way the oxidation tendency of tris-dithiolene $[Mo(S_2C_2R_2)_3]^{z-}$ decreases in the order R = H, alkyl ≈ aryl > CF_3 > CN, which in turn parallels the electron-donating and -withdrawing ability of the R substituent groups.[61,62]

Analysis of the Electronic Structure Using DFT Methods. The electronic structure of the trinuclear complexes $\mathbf{4}^{2-}$−$\mathbf{7}^{2-}$ has been investigated by means of density functional theory (DFT) calculations at the BP86/VTZP level in a gas-phase environment. The BP86 functional combined with a VTZP basis set are widely used to calculate MO energy diagrams for inorganic systems.[63] All these complexes present an idealized C_{3v} symmetry with an $^1A_1$ singlet ground state. Experimental deviations from this idealized symmetry can be attributed to packing forces because of the low energetic cost required for the folding of the dithiolene ligand. The energetic barrier associated to the folding of one dithiolene ligand has been computed by scanning the dihedral angle from 0° to 30° reaching a maximum value of 2.84 kcal/mol. Theoretically optimized bond distances are reported in Table 2, together with the experimental values. Although theoretical bond distances are systematically longer than the experimental ones, the bond lengths within each structure are well reproduced, presenting a maximum deviation of 0.09 Å.

Analysis of the molecular orbital diagram for complexes $\mathbf{4}^{2-}$−$\mathbf{7}^{2-}$ reveals a fully occupied e_1-type HOMO orbital, with an a_2-type HOMO-1 orbital lying at 0.277, 0.276, 0.175, and 0.104 eV below the HOMO for clusters $\mathbf{4}^{2-}$, $\mathbf{5}^{2-}$, $\mathbf{6}^{2-}$, and $\mathbf{7}^{2-}$, respectively. In the case of the dianionic $[Mo_3S_7(dmit)_3]^{2-}$ cluster, oxidation affords radical neutral species with a partially occupied e_1-type orbital that contains two electrons with $S = 1$. Intermolecular interactions in the $Mo_3S_7(dmit)_3$ solid results in antiferromagnetic coupling leading to a AFM state which is very close in energy to the FM state (∼20 meV).[29] The band structure diagram for the AFM state shows a small energy gap, ∼200 meV, at the Fermi level which can be associated in a first approximation to the HOMO and HOMO−1 energy difference in the cluster dianions.

Figure 3 represents the HOMO and HOMO−1 orbitals for the $[Mo_3S_7(bdt)_3]^{2-}$ ($\mathbf{5}^{2-}$) cluster dianion, where an extensive mixing between the Mo_3S_7 unit based orbitals and the dithiolene ligands based orbitals exits. Such delocalization is a direct consequence of the similar orbital energies and an adequate orbital overlap between the Mo atomic d orbitals (AO) and the p AOs of the dithiolene ligand. Interestingly, the HOMO presents a π^*-type interaction between Mo atoms and the sulfur atoms of dithiolenes whereas some bonding character can be observed among the three Mo atoms. The HOMO−1 is mainly composed of the three outer ligands and the equatorial sulfur atoms of the cluster core, without participation of Mo atoms. The same MO scheme applies for complexes $\mathbf{4}^{2-}$, $\mathbf{6}^{2-}$, and $\mathbf{7}^{2-}$, although noticeable differences in the AOs contributions from the metal and sulfur

(61) Olson, D. C.; Mayweg, V. P.; Schrauzer, G. N. *J. Am. Chem. Soc.* **1966**, *88*, 4876.
(62) Wharton, E. J.; McCleverty, J. A. *J. Chem. Soc. A* **1969**, 2258.
(63) Ray, K.; Debeer George, S.; Solomon, E. I.; Wieghardt, K.; Neese, F. *Chem.—Eur. J.* **2007**, *13*, 2783.

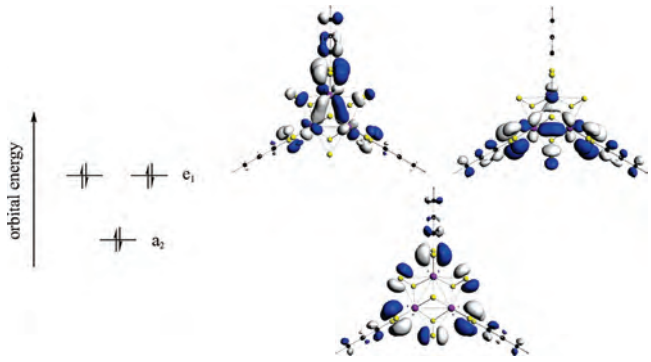

Figure 3. Representation of the HOMO and HOMO−1 orbitals for the $\mathbf{5}^{2-}$ dianion.

Table 4. Ligand and Core (Molybdenum and Sulfur) Composition (%) of the HOMO (e_1) and HOMO−1 (a_2) for clusters $\mathbf{4}^{2-}$−$\mathbf{7}^{2-}$

complex	orbital	% ligand	% Mo	% S-core
$[Mo_3S_7(tfd)_3]^{2-}$ ($[\mathbf{4}]^{2-}$)	HOMO (e_1)	65.16	27.28	7.57
	HOMO−1(a_2)	74.42	3.53	22.05
$[Mo_3S_7(bdt)_3]^{2-}$ ($[\mathbf{5}]^{2-}$)	HOMO (e_1)	61.67	29.83	8.5
	HOMO−1(a_2)	75.74	4.38	19.88
$[Mo_3S_7(dmid)_3]^{2-}$ ($[\mathbf{6}]^{2-}$)	HOMO (e_1)	77.8	16.67	5.53
	HOMO−1(a_2)	80.22	5.29	14.49
$[Mo_3S_7(dsit)_3]^{2-}$ ($[\mathbf{7}]^{2-}$)	HOMO (e_1)	82.07	14.33	3.59
	HOMO−1(a_2)	84.16	3.38	12.46

cluster core orbitals and the ligand-based orbitals are calculated as detailed in Table 4. Remarkably, ligand contributions to the HOMO vary from 61.67% for cluster $\mathbf{5}^{2-}$ to 82.07% for $\mathbf{7}^{2-}$. One has to keep in mind that magnetic and conducting properties are highly dependent on the nature of the HOMO, and as a consequence, the properties of complexes $[Mo_3S_7(\text{dithiolene/diselenolene})_3]^{2-}$ can be effectively tuned by changing the ligand taking into consideration its interaction with the cluster core. Cluster dianions with a larger contribution from the ligands to the HOMO possess a smaller energy gap between the HOMO and HOMO−1 orbitals.

While structural and electronic properties of the $\mathbf{4}^{2-}$−$\mathbf{7}^{2-}$ dianions are consistent with the indicated $Mo^{IV}{}_3$−dithiolate description, the ground states of the neutral complexes possess intriguing electronic structure problems because of the known ambiguities in the limiting descriptions of the metal and ligand oxidation states. The situation is even more complicated in delocalized cluster systems (such as the Mo_3S_7 core), where the free electron of the radical ligand is shared between one or more metal centers.

Oxidation and Physical Properties. As suggested by the cyclic voltammetry data, the full $\mathbf{4}^{2-}$−$\mathbf{7}^{2-}$ series is amenable to be easily oxidized. It is then reasonable to assume that the two waves recorded for (n-$Bu_4N)_2$[**6**] and (n-$Bu_4N)_2$[**7**] correspond to two monoelectronic electron transfer processes. However, all attempts to oxidize compounds (n-$Bu_4N)_2$[**4**] and (n-$Bu_4N)_2$[**5**] chemically (using iodine, ferrocenium salt, lead acetate, 4-iodobenzene dichloride) or electrochemically yield noncrystalline dark-fine insoluble powders whose compositions were dependent on the oxidation agent according to elemental analysis. IR spectroscopy, DC, and magnetic measurements do not provide further light on the identity of the resulting products, likely, because of the decomposition of the Mo_3S_7 trinuclear core or the dismutation of the hypothetical monoanions to give the dianion and the neutral compounds. Conversely, oxidation of compounds (n-$Bu_4N)_2$[**6**] and (n-$Bu_4N)_2$[**7**] with iodine, leads to a fine dark insoluble powder. The elemental analyses were highly reproducible, with hydrogen contents lower than 0.1% and absence of nitrogen, and were consistent with a stoichiometry corresponding to the two-electron oxidized neutral compounds, namely, **6** and **7**. As an alternative proof of the purity of the neutral solids obtained by chemical oxidation, IR measurements are also reported that supported the absence of residual oxidant or countercations in the neutral **6** and **7** solids. Consequently, we can assess with warranties that the reported elemental analysis, IR, and physical properties of neutral **6** and **7** strongly supports the purity of these neutral compounds. The same products, as judged by elemental analysis and IR, were also obtained by electrochemical oxidation from acetonitrile solutions containing the (n-$Bu_4N)_2$[**6**] and (n-$Bu_4N)_2$[**7**] salts. X-ray powder diffraction pattern of a poorly crystalline sample of **6** prepared by elecrtocrystallization matches that of the previously reported $Mo_3S_7(dmit)_3$ hexagonal phase, indicating that both phases are isostructural. The broadness of the diffraction peaks prevents us from an accurate estimation of the lattice parameters that would be severely affected by large systematic errors. This was corroborated by magnetic and conductivity measurements, as we will see later on in this section. The electronic absorption spectra in solution and solid state of the dianionic $\mathbf{6}^{2-}$ and $\mathbf{7}^{2-}$ and neutral **6** and **7** species are also investigated. Figure 4 shows the electronic absorption spectra of complexes $\mathbf{6}^{2-}$ and **6** both in the solid state and *N,N*-dimethylformamide solutions.

For the $\mathbf{6}^{2-}$ and $\mathbf{7}^{2-}$ dianions, solution electronic absorption spectra were comparable. Two bands centered at 375 and 510 nm (for $\mathbf{6}^{2-}$) and 370 and 495 nm (for $\mathbf{7}^{2-}$) are observed. The bands below 400 nm may come from the π-electronic delocalization absorption over the ligand through π−d interactions, as was observed for the (n-Me_4N)[Ni(dmid)] (380 nm),[64] whereas the lower energy bands (at ∼500 nm) are assigned to LMCT as previously observed for $[Mo_3S_7(\text{cathecolate})_3]^{2-}$ dianion.[55] An additional shoulder was observed at 335 nm for dianion $\mathbf{7}^{2-}$. Dianions $\mathbf{6}^{2-}$ and $\mathbf{7}^{2-}$ show solid-state electronic absorption spectra roughly similar to those observed in solution. The most significant difference has to do with the appearance of a shoulder to a lower energy region (650 nm for $\mathbf{6}^{2-}$ and 700 for $\mathbf{7}^{2-}$) suggesting significant interaction between cluster units in the solid state. This shift may be ascribed to the well-documented dimerization of Mo_3S_7 cluster units in which dithio- or diselenolate ligands are involved. Remarkably, the close similarities between the solid state and solution electronic absorption spectra for the $\mathbf{6}^{2-}$ and $\mathbf{7}^{2-}$ dianions are indicative of a similar MO′s scheme for both species in agreement with our theoretical calculations reported above. The solid state electronic absorption spectra of neutral **6** and **7** complexes were also very much alike. With respect to their $\mathbf{6}^{2-}$ and $\mathbf{7}^{2-}$ dianionic counterparts, the higher energy band observed

(64) Liu, S. G.; Liu, Y. Q.; Zhu, D. B. *Synth. Met.* **1996**, *79*, 49.

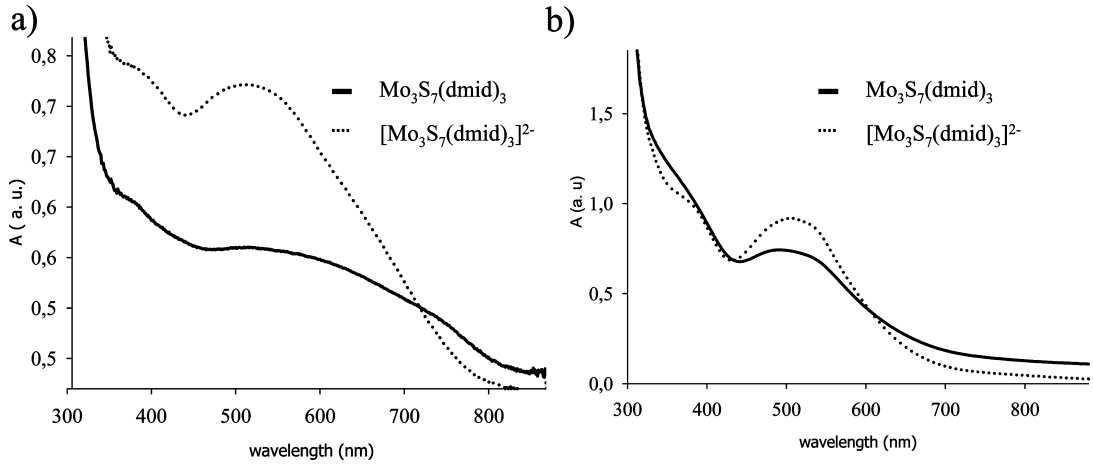

Figure 4. Electronic absorption spectra of $[Mo_3S_7(dmid)_3]^{2-}$ ($\mathbf{6}^{2-}$) and $Mo_3S_7(dmid)_3$ (**6**) (a) in the solid state and (b) in *N, N*-dimethylformamide.

(typically around ~370 nm) for the dianions remains largely unchanged in complexes **6** and **7**, whereas a significant broadening of the bands centered at ~500 nm is observed. Either for **6** and **7**, a broad shoulder is observed at lower energies (760 and 800 for **6** and **7**, respectively). These experimental evidence suggest some intermolecular interaction between neutral Mo_3S_7 complexes in the solid state.

Like the $[Mo_3S_7(dmit)_3]^{2-}$ dianion, the facile of oxidation of $\mathbf{6}^{2-}$ and $\mathbf{7}^{2-}$ dianions to their neutral **6** and **7** would result in a change from a $1a^22e^4$ to a $1a^22e^2$ ground-state configuration which leads to a partial occupation of the degenerate HOMO orbitals with the concomitant production of radicals, a prerequisite in the formation of single component molecular conductors. In addition, this two-electron oxidized molecule is also interesting from the magnetic point of view because it should have a spin $S = 1$. Because sufficiently large single crystals were not prepared, the electrical resistivities of the neutral species **6** and **7** were measured on the compressed pellets by the four-probe method. The resistivity of the neutral **6** and **7** phases increases gradually with decreasing temperature, thus indicating a semiconductor behavior. The room-temperature conductivity for **6** measured on pressed-pellets ($\sigma = 2$ S cm^{-1}, $E_a = 90$ meV) was comparable to that reported for $Mo_3S_7(dmit)_3$, while moderate conductivity was observed for **7** ($\sigma = 9 \times 10^{-2}$ S cm^{-1}, $E_a = 220$ meV). The magnetic susceptibility, measured on a polycrystalline sample, shows a continuous decrease in the χT versus T plot upon cooling (Figure 5). At room temperature the χT values are clearly below the value expected for a spin triplet (~1 emu K mol^{-1}). This low room-temperature value, together with the significant decrease in χT, indicate the presence of antiferromagnetic exchange interactions between the unpaired electrons of the neutral **6** and **7** molecules. Given the similarities between the magnetic properties of compounds **6** and **7** and the dmit derivative (see Figure 5), we can anticipate that the magnetic behavior of these compounds must be very similar and, therefore, that they can be well explained as a one-dimensional exchange network formed by randomly distributed $S = 0$ and 1 spins.[29]

In conclusion, the hexagonal phases **6** and **7**, as well as the previously reported $Mo_3S_7(dmit)_3$, represent new single-component molecular conductors built by magnetic units.

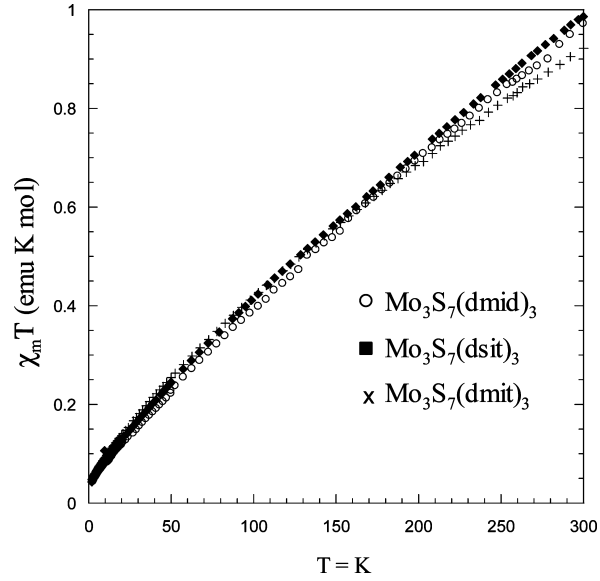

Figure 5. $\chi_m T$ vs T for polycrystalline samples of $Mo_3S_7(dmit)_3$,[29] $Mo_3S_7(dmid)_3$ (**6**), and $Mo_3S_7(dsit)_3$ (**7**).

In the case of $Mo_3S_7(dmit)_3$, a very small energy gap is calculated at the Fermi level, something that harmonizes with the activated, although high, conductivity of these systems. The origin of this low energy gap is closely related to the small energy difference between the HOMO and HOMO−1 orbitals in the dianionic clusters employed as precursors.

Conclusions

A series of tris-dithiolate complexes based on the C_{3v} symmetry trinuclear Mo_3S_7 cluster unit are conveniently synthesized starting from the bromine $[Mo_3S_7Br_6]^{2-}$ dianion and the corresponding tin salts of general formula (n-Bu)$_2$Sn(dithiolate). This synthetic route affords the dianionic $[Mo_3S_7L_3]^{2-}$ complexes: $\mathbf{4}^{2-}$ (L = tfd (bis(trifluoromethyl)-1,2-dithiolate), $\mathbf{5}^{2-}$ (L = bdt (1,2-benzenedithiolate), and $\mathbf{6}^{2-}$ (L = dmid (1,3-dithia-2-one-4,5-dithiolate) in moderate to high yield. The diselenolate $\mathbf{7}^{2-}$ cluster dianion (where L = dsit (1,3-dithia-2-thione-4,5-diselenolate) is prepared starting from the zinc $[Zn(dsit)_2]^{2-}$ precursor. The structural and electrochemical features of these complexes further complement the knowledge of previously reported homologous

Mo_3S_7 complexes with dithiolate (L = mnt, tdas, and dmit) ligands.[29,49,50] The electrophilic character of the axial sulfur present in the Mo_3S_7 unit results in the formation of supramolecular aggregates. Coordination of redox active ligands to the Mo_3S_7 unit awards these complexes with electrochemical activity in the oxidation region where one to two redox processes can be distinguished depending on the nature of the outer ligand. DFT calculations suggest that oxidation removes electrons from a doubly occupied e-symmetry orbital, which is delocalized over the ligand and the Mo_3S_7 cluster core. The calculated small energy values between the HOMO and HOMO−1 gap (from 0.114 to 0.277 V) makes this system ideal for the preparation of single-component molecular conductors based on magnetic cluster units. In fact, chemical or electrochemical oxidation of the dmid and dsit derivatives $\mathbf{6}^{2-}$ and $\mathbf{7}^{2-}$, affords neutral species as microcrystalline or amorphous solids, depending on the reaction conditions. Both **6** and **7** present effective magnetic moments close to 1 μB indicative of high spin states (S = 1) and moderate electrical conductivities, $\sigma_{rt} = 2$ S cm^{-1} (**6**) and $\sigma_{rt} = 9 \times 10^{-2}$ S cm^{-1} (**7**) with a semiconducting behavior.

Acknowledgment. This work was made possible through the support of the French Spanish Integrated Action program PICASSO (Nos. 11445PL and HF-2005-0146), the Spanish Ministerio de Educación y Ciencia (MEC, Project CTQ2005-09270-C02-1), Generalitat Valenciana (GV/2007/106), Fundació Caixa Castelló-Bancaixa (Grant P1.1B2007-12), and the European Unión (COST Action D35-WG-0011-05). V.P. thanks the Juan de la Cierva program from the MEC for support. The authors are grateful to the Serveis Centrals d'Instrumentació Científica (SCIC) of the Universitat Jaume I for providing us with spectroscopic and X-ray facilities. We also thank Prof. S. Uriel from the University of Zaragoza for providing us with some samples of the (n-Bu)$_2$Sn(dsit) precursor.

Supporting Information Available: Crystallographic data (excluding structure factors) for the structures reported in this paper.This material is available free of charge via the Internet at http://pubs.acs.org.

IC8009546